



HAL
open science

FLUCTUATIONS IN THE COMPOSITION OF LATE MIOCENE CALCAREOUS NANNOFOSSIL ASSEMBLAGES AS A RESPONSE TO ORBITAL FORCING

Luc L Beaufort, Marie-Pierre Aubry

► **To cite this version:**

Luc L Beaufort, Marie-Pierre Aubry. FLUCTUATIONS IN THE COMPOSITION OF LATE MIOCENE CALCAREOUS NANNOFOSSIL ASSEMBLAGES AS A RESPONSE TO ORBITAL FORCING. *Paleoceanography*, 1990, 5 (6), pp.845-865. 10.1029/PA005i006p00845 . hal-01460402

HAL Id: hal-01460402

<https://hal.science/hal-01460402>

Submitted on 2 Feb 2021

HAL is a multi-disciplinary open access archive for the deposit and dissemination of scientific research documents, whether they are published or not. The documents may come from teaching and research institutions in France or abroad, or from public or private research centers.

L'archive ouverte pluridisciplinaire **HAL**, est destinée au dépôt et à la diffusion de documents scientifiques de niveau recherche, publiés ou non, émanant des établissements d'enseignement et de recherche français ou étrangers, des laboratoires publics ou privés.

FLUCTUATIONS IN THE COMPOSITION OF LATE
MIOCENE CALCAREOUS NANNOFOSSIL
ASSEMBLAGES AS A RESPONSE TO ORBITAL
FORCING

Luc Beaufort and Marie-Pierre Aubry

Département des Sciences de la terre,
Université Lyon I, Villeurbanne, France and
Woods Hole Oceanographic Institution, Woods
Hole, Massachusetts

Abstract. Fluctuations in abundance between the two calcareous nannofossil species *Coccolithus pelagicus* and *Reticulofenestra pseudumbilica* are observed in the upper Miocene sediments recovered from Deep Sea Drilling Project hole 552A. A record of these fluctuations (Cp/Rp) is established for a time interval of ~1.35 m.y. (from 4.9 to 6.25 Ma) and is shown to yield periodicities which correspond to Milankovitch periodicities. A change in regime occurred at 5.72 Ma, as indicated by a shift from a series dominated by the 20-kyr cycle to a series dominated by the 100-kyr cycle. The Cp/Rp is compared with the isotopic $\delta^{18}\text{O}$ and $\delta^{13}\text{C}$ records from benthic and planktonic foraminifera. It is shown that a good correlation between the Cp/Rp and the isotopic records occurs only at times of major global changes. This suggests that the Cp/Rp, which reflects water masses movements, yields a complex paleoclimatic/paleoceanographic message which can help improving our understanding of the late Miocene history.

INTRODUCTION

The geographic distribution of the calcareous nannoplankton, which represents an important part of the modern phytoplankton, is essentially linked to environmental parameters (see overview by Tappan [1980]). Its fossil representatives, the calcareous nannofossils, have been shown to be useful for paleoclimatic reconstructions. McIntyre and Bé [1967] were among the first authors to recognize that during the Pleistocene, the composition of coccolith assemblages reflected sea surface temperatures (SST) and was changing with latitude. Calcareous nannofossils have been used in an attempt to study climatic evolution through the Paleogene [Haq and Lohmann, 1976; Haq et al., 1977] and the Miocene [Haq, 1980; Lohmann and Carlson, 1981]. More recently, Backman et al. [1986] and Backman and Pestiaux [1987] found that fluctuations in the absolute abundance of the Pliocene discoasters yield periodicities which may correspond to the Earth orbital parameter cycles.

At North Atlantic Deep Sea Drilling Project hole 552A, two species, *Coccolithus pelagicus* and *Reticulofenestra pseudumbilica*, alternatively dominate in the late Miocene calcareous nannofossil assemblages [Keigwin et al., 1986]. Similar fluctuations between these two taxa are observed in other late Miocene assemblages from geographically broadly separated regions (e.g., Kerguelen

Copyright 1990
by the American Geophysical Union.

Paper number 90PA01880
0883-8305/90/90PA-01880\$10.00

plateau in the Southern Indian ocean [L. Beaufort and M.-P. Aubry, submitted manuscript, 1990]; Rio-Grande Rise, South Atlantic Ocean, (M.-P. Aubry (personal observation, 1987) and see Haq and Berggren [1978, Figure 5]); and Crete, Mediterranean sea [Schmidt, 1979]).

In an attempt to decipher the paleoclimatic/paleoceanographic significance of these fluctuations, a detailed record of the variations in the ratio between the two species *C. pelagicus* and *R. pseudoumbilica* in the upper Miocene sediments recovered from DSDP hole 552A has been established and investigated using time series analysis. It is hoped that this record will contribute to improve our understanding of the late Miocene history, a period of complex oceanographic and climatic evolution which witnessed a general regression [Kennett, 1967], a major extension of the Antarctic ice cap [Shackleton and Kennett., 1975] and the dessication of the Mediterranean sea [Nesteroff et al., 1972; Hsü et al., 1973].

METHODOLOGY

DSDP site 552 is located on Rockall bank (56°N, 10°S) in the North Atlantic Ocean

(Figure 1). Lithologic homogeneity, minor bioturbation, very high abundance in calcareous nannofossils (70-90% of the sediment) and relatively high and constant CaCO_3 content (91-96%) [Roberts et al., 1984] make the upper Miocene calcareous nannofossil oozes and chalks recovered from DSDP hole 552A particularly suitable for studying variations in composition of calcareous nannofossil assemblages.

Most quantitative studies of calcareous nannofossil assemblages aiming at paleoceanographic reconstructions have taken into account all species within the assemblages [e.g., Haq and Lohmann, 1976; Lohmann and Carlson, 1981; Haq, 1980; Pujos, 1985]. A different approach consists in studying the variation in abundance within a group. Such an approach was followed by Backman et al. [1986] and Chepstow-Lusty et al. [1989], who studied abundance variations between species of the genus *Discoaster* in Pliocene sediments from the North Atlantic. These authors followed the methodology described by Backman and Shackleton [1983] which consists of counting all specimens of a chosen species in a number of view fields until an "appropriate" number of specimens is obtained, the abundance of the species

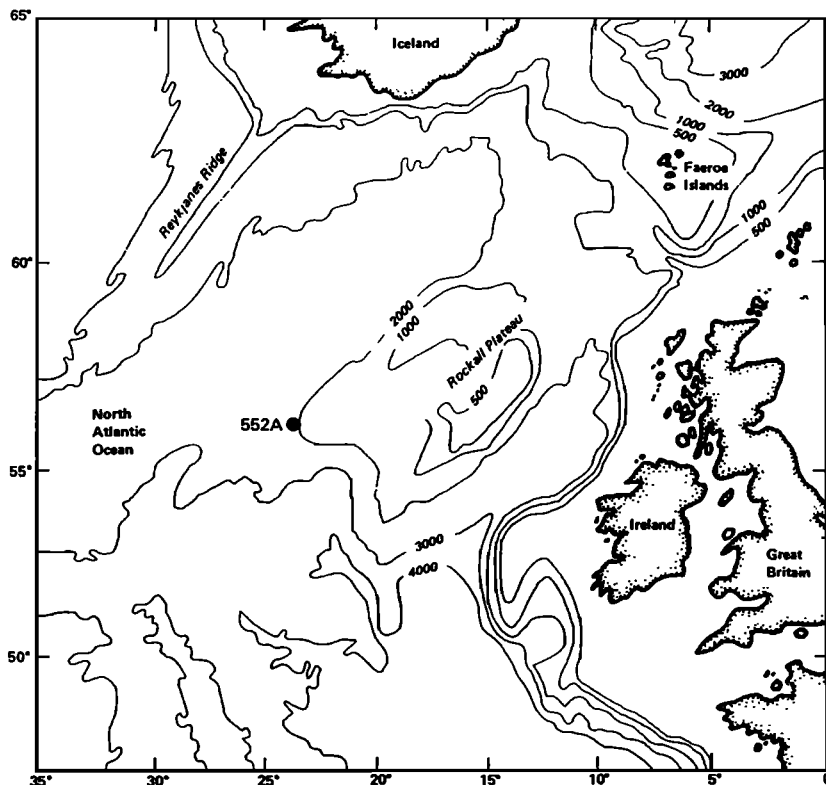


Fig. 1. Geographic location of DSDP site 552.

being then expressed relative to unit area of the slide scanned. This methodology was not followed in this study for several reasons. First, the absolute abundance of a taxon in sediments varies through time not only as a function of its own sedimentation rate but also as a function of the sedimentation rates of other taxa as well as of nonbiogenic components in the sediments, both factors leading to the dilution of the considered taxon. Second, the number of fields to be counted in order to obtain an "appropriate" number of specimens varies with the concentration of a preparation, so that the absolute abundance of taxa cannot be obtained accurately. Third, discoasters are extremely rare in the sediments studied from site 552 (in most instances, no discoasters were encountered while counting 300 specimens of *C. pelagicus* and *R. pseudoumbilica*), and although discoasters are usually considered as warm water indicators, there are indications that some may be indicative of cooler waters [Bukry, 1971].

A more accurate determination of the temporal variation in abundance of a taxon is to study changes in its abundance relative to that of another well-chosen taxon, in which case the differential sedimentation rates between the taxa involved are the only factor of variation. *Coccolithus pelagicus* and *Reticulofenestra pseudoumbilica* constitute the bulk of the assemblages in the interval studied with percentages averaging 90% (between 104 and 150 m below sea floor (mbsf), cores 552A-23 to 32) (Table 1). Coccoliths in both species are of about the same size and shape and are placoliths, a group of coccoliths most resistant to dissolution. For these reasons, the relative frequencies between the two species are unlikely to be biased by differential physical (e.g., winnowing) or chemical (e.g., dissolution) processes. In this study, the concept of *Reticulofenestra pseudoumbilica* is taken in a broad sense following the suggestion that forms which have been distinguished based solely on size differences [e.g., Pujos, 1987; Driever, 1988] may represent different morphotypes of *R. pseudoumbilica* rather than different species [Beaufort, 1989]. Among the other taxa present, the most frequent are *Calcidiscus leptoporus*, *C. macintyreii*, *Helicosphaera carteri*, and some species of the genus *Discoaster*, in particular, *D. brouweri*, *D. challengerii*, *D. quinqueramus*, *D. variabilis*, and *D. surculus* [see Backman, 1984, Table 2, p. 412]. Except for *C. leptoporus* which percentage raises up to 10% at some levels, none of the other taxa constitute more than 2% of the assemblages at any level.

TABLE 1. Percentage of *Coccolithus pelagicus* + *Reticulofenestra pseudoumbilica* in Randomly Taken Samples From the Interval Studied

Depth	% Cp+Rp/tot
105	93
107.96	92
109.12	81
112.02	90
114.55	93
117.09	93
119.52	91
122.51	95
124.51	87
127.54	96
129.53	83
131.53	76
134.55	79
137.55	90
139.5	92
142.5	90
144.5	85
147.5	90
149.5	94
152.5	89

The percentage of both species is high at all levels and average 90%.

In order to obtain a very detailed record of the variations of the relative abundances of *C. pelagicus* and *R. pseudoumbilica* during the late Miocene, samples were taken every 10 cm in cores 552A-23 to 28-1 (between 104 and 130 mbsf) and every 5 cm in cores 552A-28-2 to 32 (between 130 and 150 mbsf), providing a time resolution of at least 3000 years. Smear slides were prepared from all samples. The two species were counted in each slide under the light microscope until a total of 300 specimens was reached. The percentage of *C. pelagicus* versus *R. pseudoumbilica* (Cp/Rp) was calculated as follows: {number of *Coccolithus pelagicus* / (number of *R. pseudoumbilica* + number of *C. pelagicus*)} X 100. This is referred to as the "Cp/Rp" in the text. The Cp/Rp fluctuates widely between 4 and 95% (Figure 2 and Table 2).

STRATIGRAPHY/CHRONOLOGY

The stratigraphy of the upper Miocene interval recovered from DSDP hole 552A was established through integrated magnetostratigraphy, biostratigraphy and isotope stratigraphy [Keigwin et al., 1986; Keigwin, 1987], so that a precise chronology can be derived.

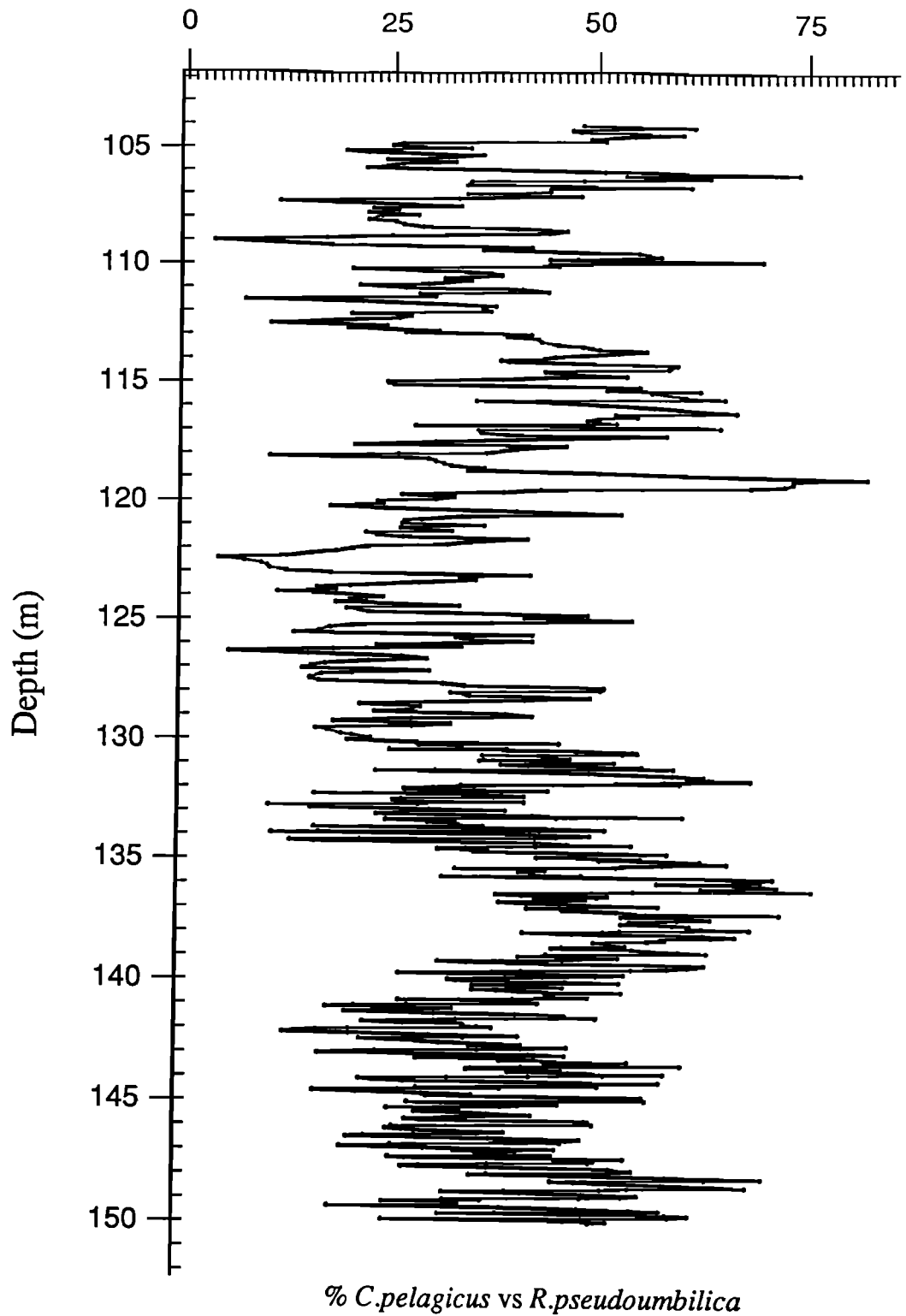


Fig. 2. Fluctuations in abundance of *Coccolithus pelagicus* versus *Reticulofenestra pseudoumbilica* in the upper Miocene sediments recovered from DSDP hole 552A.

TABLE 2. Values of the Cp/Rp in the Samples Analysed in This study

Depth	Cp/Rp	Depth	Cp/Rp
104.01	48	109.01	3.3
104.1	61.3	109.1	10.5
104.22	46.7	109.2	17.2
104.3	47.7	109.3	41.7
104.4	59.9	109.41	35.8
104.49	54.2	109.55	54.7
104.6	49	109.7	57.3
104.7	50.7	109.77	47.3
104.8	25.9	109.8	44
104.9	24.7	109.9	69.3
105.01	34.2	110.01	44
105.1	19	110.1	45
105.2	21.7	110.2	19.8
105.3	35.7	110.34	34
105.4	31.3	110.4	36.7
105.5	24	110.49	38
105.6	32.3	110.61	31
105.69	25.8	110.7	34.3
105.86	21.5	110.85	29
105.9	28.7	110.91	20.7
106.01	50.6	111.01	26.3
106.14	73.7	111.08	40.6
106.2	53.2	111.2	43.8
106.3	63.1	111.26	28
106.41	48	111.38	29.8
106.44	34.3	111.5	7
106.6	33.8	111.6	21
106.7	60.9	111.7	31
106.8	44	111.8	37.3
106.9	44	111.85	35.7
107	33.8	112.01	36.7
107.09	47.7	112.11	19.7
107.2	32.7	112.2	26.9
107.3	11	112.3	25.5
107.4	21	112.41	17.7
107.52	33	112.52	10
107.61	22.3	112.62	24
107.7	25.3	112.72	19.3
107.8	21.7	112.84	30.3
107.91	27.7	112.9	26.3
107.96	23.3	113.01	41.7
108.11	21.7	113.1	38.8
108.2	25	113.2	42.6
108.3	26	113.31	43
108.4	28.3	113.41	45
108.5	39.9	113.51	48
108.6	46	113.61	50
108.7	43.9	113.7	55.6
108.8	24.6	113.78	52.3
108.9	16.6	113.93	44.6
114.01	43.4	19.03	81.8
114.08	38	19.13	73
114.12	39	19.23	73
114.29	59.3	19.33	72
114.44	58.3	19.42	68
114.55	43.5	19.52	43

TABLE 2. (Continued)

Depth	Cp/Rp	Depth	Cp/Rp
114.68	48	19.62	38.4
114.74	53.3	19.72	26
114.76	46	19.82	32.3
114.88	38.2	19.92	30
114.98	24.2	20	23
115.1	25	20.1	23.7
115.2	54.9	20.22	17.3
115.31	51	20.3	24
115.36	62	20.42	40
115.43	56.3	20.53	52.7
115.6	60.3	20.64	33.3
115.7	64.9	20.76	28.3
115.76	35	20.82	26.3
115.8	42.6	20.92	26
116.03	56.6	21.03	36
116.11	59.6	21.12	25.8
116.26	66.3	21.26	32
116.33	52	21.32	21.6
116.44	54.6	21.42	23
116.5	50	21.5	26.1
116.6	48.6	21.59	41.3
116.7	52.1	21.71	34.3
116.8	27.6	21.82	31.5
116.85	61.7	21.92	21.7
116.9	64.4	22	20
116.99	35.3	22.1	18
117.09	35.6	22.2	15
117.2	38.8	22.32	12
117.24	58	22.42	4
117.4	40	22.52	7
117.5	30	22.62	9
117.62	20.2	22.72	9.7
117.67	46	22.82	10
117.8	40	22.92	12
117.98	36.3	23.02	17.3
118.01	25.5	23.12	41.7
118.1	10	23.2	33
118.2	29.1	23.32	35
118.3	30	23.42	28
118.4	31	23.57	19.7
118.5	32	23.62	15.7
118.6	36	23.72	18
118.7	34	23.82	11
118.8	50	23.9	18
118.9	60.2	24.03	23.7
124.12	19.7	129.23	17.8
124.22	21.7	129.32	32
124.25	18	129.42	27.3
124.41	33	129.53	15.7
124.51	19.3	129.6	17
124.66	22	129.74	18.7
124.72	33	129.8	20
124.81	48.7	129.92	22.3
124.91	41	130.01	19.5
125.01	54	130.1	27.9
125.11	37	130.14	45.3
125.22	20	130.21	28.2

TABLE 2. (Continued)

Depth	Cp/Rp	Depth	Cp/Rp
125.31	17.3	130.28	33.5
125.43	16	130.33	33
125.53	13	130.36	39
125.62	42	130.4	24.7
125.72	32.6	130.45	47.5
125.82	34.7	130.5	54.2
125.89	42	130.55	54.7
126.04	23	130.58	53
126.12	33.3	130.63	36
126.22	17.7	130.68	45
126.34	5.3	130.73	45
126.42	14.7	130.77	46.7
126.52	26	130.82	36.2
126.61	29	130.86	35.7
126.72	22	130.93	52
126.84	16.7	130.97	47.3
126.94	15	131.02	38.3
127.02	14	131.06	41.7
127.12	29.3	131.1	55.3
127.22	20	131.15	51
127.27	16.3	131.2	59
127.42	14.9	131.25	30.2
127.54	16	131.28	23
127.64	31	131.37	49
127.74	33.7	131.42	54.3
127.82	50.7	131.47	58.9
127.92	50.3	131.52	62.6
128.02	32	131.58	60.7
128.09	34	131.63	63.2
128.14	34.3	131.68	68
128.24	49	131.73	58
128.34	41.1	131.78	52.3
128.52	21	131.83	59.7
128.62	28.3	131.88	33.4
128.72	27.3	131.93	35
128.82	22.8	131.98	30
128.92	38.8	132.03	26.5
129.02	42	132.08	26.6
129.12	27.3	132.13	44
132.18	38.4	134.71	50.2
132.23	28.5	134.76	58.3
132.26	15.6	134.81	46.8
132.31	36.5	134.86	47.4
132.36	41.1	134.91	42.8
132.41	37.4	134.96	55.2
132.46	26.1	135.01	50.3
132.51	25.1	135.06	62.2
132.56	25.4	135.11	57.8
132.61	41.1	135.16	65.3
132.66	29.1	135.21	57.8
132.71	28.1	135.26	53.1
132.76	10.1	135.31	52.3
132.81	17.6	135.36	32.7
132.86	15.1	135.41	42.7
132.91	29.5	135.46	43.8
132.96	38.8	135.51	40.5
133.01	26.9	135.56	42.1

TABLE 2. (Continued)

Depth	Cp/Rp	Depth	Cp/Rp
133.06	26.1	135.61	42.5
133.11	23.1	135.66	48.1
133.17	42.2	135.71	31.1
133.21	60.1	135.76	70.7
133.26	45.1	135.81	67.9
133.31	24.3	135.86	66.3
133.36	24.2	135.91	69.3
133.41	32.7	135.96	57.2
133.46	29.3	136.01	66.6
133.51	32.1	136.06	69.4
133.56	33.1	136.1	71.2
133.61	36.1	136.16	62.4
133.66	15.6	136.2	62.4
133.71	44.7	136.27	75.3
133.76	50.9	136.31	54.4
133.81	43.1	136.43	37.8
133.86	16.1	136.47	41
133.91	10.5	136.5	51.3
133.96	41.9	136.55	50.1
134.01	49.1	136.6	42.5
134.06	45.1	136.65	48.7
134.11	42.5	136.7	46.1
134.16	21.1	136.75	38.2
134.21	12.7	136.8	41.6
134.26	15.6	136.92	57.3
134.31	42.6	136.97	45.6
134.36	46.4	137.01	41.6
134.41	54.1	137.06	48.8
134.46	42.7	137.1	46
134.51	34.1	137.15	52.4
134.56	30.6	137.2	54
134.61	36.7	137.24	71.5
134.66	35.1	137.3	53.7
137.35	53	139.96	32
137.4	61	140.01	33
137.45	63.4	140.06	46.3
137.5	59.6	140.11	52.7
137.55	54	140.16	40.3
137.61	57	140.21	35
137.65	53	140.26	44
137.7	59	140.31	46
137.73	61	140.36	35
137.78	60.8	140.41	38
137.83	62.4	140.46	41
137.88	68	140.51	53
137.94	52.8	140.56	44
137.98	50.8	140.61	44
138.01	41.1	140.66	44.8
138.06	47.1	140.71	49
138.11	62.6	140.76	40
138.16	66.3	140.81	26
138.21	63.6	140.86	42
138.26	57.8	140.91	37.5
138.31	58.1	140.96	43
138.36	56.1	141.01	27
138.41	49.7	141.06	20.6
138.56	53.5	141.11	17.2

TABLE 2. (Continued)

Depth	Cp/Rp	Depth	Cp/Rp
138.61	45.9	141.16	32.5
138.66	44.7	141.21	28.9
138.71	54.3	141.26	24.3
138.76	56.3	141.31	19.5
138.81	59.7	141.36	30.3
138.86	63	141.41	40.3
138.91	44	141.46	46
138.96	48	141.51	46.3
139.01	40.6	141.56	50
139.06	52.6	141.61	33
139.11	48	141.66	30.3
139.16	46	141.71	21.7
139.21	30.7	141.76	26.6
139.26	34.3	141.81	33.7
139.31	44	141.86	34
139.36	62.7	141.91	35.7
139.41	61.8	141.96	37.4
139.46	60.8	142.01	20
139.51	58.4	142.06	16.1
139.56	54.2	142.11	13.5
139.61	41	142.16	12.1
139.66	37.5	142.21	20
139.71	26	142.26	29.7
139.76	53.3	142.31	40.6
139.81	50	142.36	34
139.86	43.6	142.41	21.3
139.91	39.1	142.46	24.8
142.51	29	145.06	31.3
142.56	30.9	145.11	45.5
142.61	36.4	145.16	40.7
142.66	41	145.21	38.6
142.71	34.7	145.26	24.8
142.76	46.5	145.31	33.6
142.81	41	145.36	33
142.86	35.7	145.41	28.1
142.91	23.3	145.46	35
142.96	21	145.51	37
143.01	16.3	145.56	42.3
143.06	42	145.61	34
143.11	46.3	145.66	32
143.16	32.2	145.7	27
143.21	28.2	145.76	29
143.26	42.6	145.81	48.8
143.31	38.4	145.86	49.2
143.36	53.8	145.91	47.8
143.41	44	145.96	49.7
143.46	44	146.01	25.4
143.51	60	146.06	27.8
143.56	41.1	146.11	24.7
143.61	34.9	146.16	26.6
143.66	34.4	146.21	30.7
143.71	45.9	146.26	39

TABLE 2. (Continued)

Depth	Cp/Rp	epth	Cp/Rp
143.76	39.4	146.31	35.8
143.81	46.8	146.36	28.1
143.86	58	146.41	22
143.91	51	146.46	19.9
143.96	42	146.51	37.2
144.01	32	146.56	48.2
144.06	21.3	146.61	46.6
144.11	23	146.66	38.1
144.16	26.7	146.71	45.9
144.21	57.5	146.76	25.3
144.26	43.5	146.81	29.4
144.31	47.2	146.86	19.1
144.36	50.3	146.91	29.2
144.41	28.3	146.96	45.2
144.46	38.5	147.01	32.9
144.51	26.1	147.06	40.5
144.56	15.8	147.11	35.6
144.61	21	147.16	36.6
144.66	29	147.21	44.8
144.71	35	147.26	25
144.76	29.5	147.31	27
144.81	55.5	147.36	53.4
144.86	48.7	147.41	45.3
144.91	46	147.46	49.8
144.96	55.9	147.51	49.3
145.01	27.2	147.56	37.1
147.61	28.7	148.86	55
147.66	26.6	148.91	53.2
147.71	37	148.96	48.3
147.76	51.7	149.01	31.6
147.81	52.2	149.06	36.2
147.86	54.4	149.11	24.3
147.91	51.6	149.16	31.7
147.96	37	149.21	33.5
148.01	34.9	149.26	32.5
148.06	51.9	149.31	17.7
148.11	58.4	149.36	38.6
148.16	69.5	149.4	48
148.21	63	149.46	54.2
148.26	44.8	149.51	57.6
148.31	47.6	149.56	38.1
148.36	52	149.6	31
148.41	58	149.66	58.4
148.46	64	149.71	61
148.51	67.7	149.76	58.7
148.56	54	149.81	48.5
148.61	50.7	149.86	24.3
148.66	39.2	149.91	46.3
148.71	31.5	149.96	51.4
148.76	41.1	150.01	49.3
148.81	48.6		

Magnetostratigraphy provided reliable data for the Pliocene and Pleistocene section recovered from this hole [Shackleton et al., 1984] and the Gauss/Gilbert boundary was identified in core 552A-12. A high-resolution magnetostratigraphy was also obtained for the upper Miocene interval (cores 552A-26 to 32; 120 to 150 mbsf) [Keigwin et al., 1986], but because of uninterpretable magnetic data in cores 13 to 25, there was some question as to the identification of Chron 5 [Keigwin et al., 1986]. Isotope stratigraphy [Keigwin, 1987] allowed resolution of this uncertainty, so that the record can be confidently interpreted as Chron 6 and the entire Chron 5. The normal/reverse boundaries which occur at 150, 142, and 125 mbsf correspond to chrons 6N/6R, chrons 6R/5bN, and Chron 5aN/Gilbert boundaries, respectively. These yield respective estimated ages of 6.37 Ma, 5.89 Ma, and 5.35 Ma [Berggren et al., 1985].

The Miocene/Pliocene boundary provides an additional tie point for age control in this study. Although not confirmed [Keigwin et al., 1986], the occurrence of the calcareous nannofossil species *Ceratolithus acutus* at 104 mbsf (in core 552A-22-CC) [Backman, 1984] indicates a level close to the Miocene/Pliocene boundary [see Perch-Nielsen, 1985]. The highest occurrence of the diatom *Thalassiosira miocenica* at 104 mbsf and the lowest occurrence of *T. oestrupii* at 98 mbsf also approximate the Miocene/Pliocene boundary [Badlauf, 1984]. Keigwin [1987] interpreted the maximum peak in $\delta^{18}\text{O}$ values which occurs at 106 mbsf as reflecting the last cooling event of the late Miocene which contributed to the Messinian salinity crisis [Hodell and Kennett, 1986].

The age of the base of the Zanclean stage (i.e., the age of the Miocene/Pliocene boundary) has been determined using different methodologies. Zijdeveld et al. [1986] studied the magnetostratigraphic records of the sections of Singa and Roccella in Calabria and estimated the age of the Miocene/Pliocene boundary at 4.83 Ma based on a simple extrapolation of the sedimentation rate calculated for the upper part of the section. A similar magnetostratigraphic record was obtained from the section of Capo Spartivento also in Calabria [Channell et al., 1988]. In order to date the base of the Zanclean which lies a few meters below the lowest reversal at Capo Spartivento, Channell et al. [1988] assumed periodical calcareous/marl alternations (~19 kyr cycle) and calculated the sedimentation rate in the lower part of the section. They inferred an age of 4.93 Ma. This age is preferred here

because the use of cyclicity as a "chronometer" does not seem unreasonable when cycles are particularly well defined. Moreover, the main error which could ensue from such practice would result in a younger age due to missing cycles. It appears therefore that the age of the Miocene/Pliocene boundary is at least 4.93 Ma. Assuming that this age is correct and that the youngest $\delta^{18}\text{O}$ maximum in both benthic and planktonic foraminifera which occurs at 106 mbsf in DSDP hole 552A correlates with the Miocene/Pliocene boundary [Keigwin, 1987], a very precise calibration point is obtained.

The age model on which spectral analysis is based in this study is given in Figure 3, and the tie points used to establish it are summarized in Table 3. The record of fluctuations in abundance of *C. pelagicus* and *R. pseudoumbilica* is about 1.5 m.y. long (from 4.9 Ma to 6.25 Ma) and corresponds to the entire Messinian.

TIME SERIES ANALYSIS

Standard time series analysis procedures have been followed to estimate the power spectral density as a function of frequency [Shumway, 1988]. Through interpolation by a cubic splines routine, the raw data were transformed in a new series equally spaced at 3 kyr (the average time spacing between consecutive samples). The resulting series (Figure 4) was smoothed by a 3-point moving average and completed by zeros padding to 1024 points. A discrete Fourier transform (DFT) was computed using a cosine taper and a 9-point smoothing.

Seven major peaks occur in the power spectrum (Figure 5 and Table 4). They are at 438, 91, 41, 30, 24, 21, and 15.6 kyr. As a result of variations in the sedimentation rate between calibration points, the imperfection of our estimated best chronology limits the accuracy of the frequency estimates. Nevertheless, several of these peaks are very close to the Milankovitch cycles: 438 kyr compares with 413 kyr (the first term of the eccentricity) and 91 kyr compares with 95 kyr (the second term of the eccentricity). Usually, the combined second and third (123 kyr) terms of the eccentricity produces a 100-kyr period, so that 91 should be compared to 100. The 41 kyr corresponds to the first term of the obliquity parameter. The 24 and 21 kyr are close to 23 and 19 kyr, which represent the main terms of the precession parameters.

Additional periods occur. The 30-kyr period was also observed in Pleistocene series from equatorial Pacific cores [Pisias and Rea,

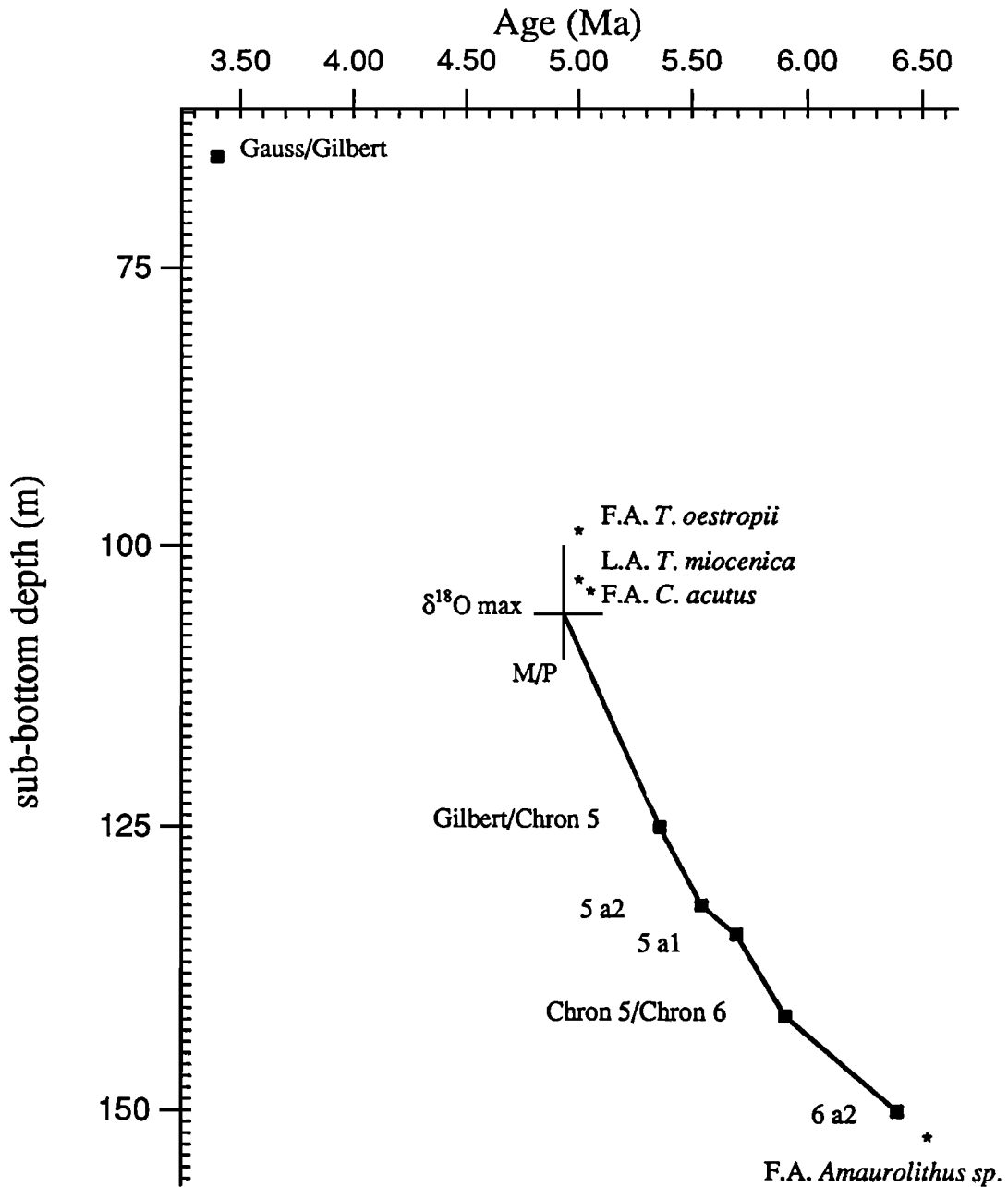


Fig. 3. Chronologic model used in this study. The thick line links the selected tie-points (see Appendix 1). Stars, biostratigraphic markers. Squares, magnetic reversal boundaries. Age of the Miocene/Pliocene boundary as estimated by Channel et al. [1988].

1988]. Arguing that this period was found "in other well-dated paleoclimatic record [J. Imbrie, personal communication 1987]" Pisias and Rea [1988, p. 32] explained this period as a nonlinear response from the 100 kyr and the 41 kyr, which gives a period of 29 kyr

(frequency of $1/100,000 + 1/41,000$). Similarly, the 15-kyr period could represent a nonlinear response of the 41-kyr and 23-kyr cyclicities which give a 14.7-kyr period [Le Treut et al., 1988].

Band-pass filters have been successfully

TABLE 3. Tie Points Used to Establish the Chronological Model Used in This Study

Events	Stratigraphic Level, mbsf	Estimated Age
FAD <i>T. oestrupii</i> (1)	98.14	Mio-Pliocene B. (1)
FAD <i>C. acutus</i> (2)	104	5.0 Ma (3)
LAD <i>T. miocenica</i> (1)	104	Mio-Pliocene B. (1)
$\delta^{18}\text{O}$ maximum (4)	106	Mio-Pliocene B. (5)
Gilbert/Chron 5 (4)	124.44-125.49	5.35 Ma (3)
Chron 5a1/Chron 5N (4)	131.97-132.25	5.53 Ma (3)
Chron 5N/Chron 5a2 (4)	134.49-134.75	5.68 Ma (3)
Chron 5/Chron 6 (4)	141.94-141.98	5.89 Ma (3)
Chron 6/Chron 7 (4)	149.94-150.25	6.37 Ma (3)
FAD <i>A. primus</i> (4)	152	6.5 Ma (3)

References: (1) from Badlauf [1984], (2) from Backman [1984], (3) from Berggren et al. [1985], (4) from Keigwin et al. [1986], (5) from Keigwin [1987].

used to sort out the respective strength of the Milankovitch periodicities [e.g., Ruddiman et al., 1989]. Three linear filters centered on frequencies of 1/100, 1/41, and 1/22 kyr (for 1/24 to 1/19 kyr) and a low-pass filter cutting at 1/200 kyr were designed following the methodology of Shumway [1988]. Figure 6 shows the filtered series. The percent of the total variance of each filtered series is given in Table 3. The importance of the low frequencies is obvious. This dominance was already seen in the periodogram. The 438-kyr period in the periodogram (Figure 5) is hardly detectable in the low-pass-filtered series. Resolution in the periodogram is low in the lowest frequencies, and the peak at 1/438 results, in fact, from the nonstationary behavior of the original series. In the series filtered at 100 kyr, clear 100-kyr cycles with large amplitude (about 20%) occur in the younger part of the series (younger than 5.7 Ma). The ages of these cycles are given in Figure 4. In the lower part of the series, the 100-kyr filtered series correlates with the low-pass-filtered series. Periods of 41 kyr are of about equal amplitude in the series except for a significant increase at 5.22 Ma as a result of a large increase in abundance of *C. pelagicus*. The 23- to 19-kyr period appears to decrease through time. In the oldest part of the record (6.3-5.8 Ma) the signal is regular

and of large amplitude. In the younger part of the series (5.9-5 Ma) the signal is less regular and weaker. This difference between the older and younger parts of the series can be seen in the frequency domain through separate spectral analysis of these two parts. For this, the statistical method outlined above was used but with a shorter zero padding (each subseries being shorter, ~240 points) and a 7-point average smoothing. Figure 7 shows the power density spectrum of both subseries. The solid line corresponds to the spectrum of the younger subseries, from 5.72 to 4.89 Ma; the dashed line corresponds to the spectrum of the older subseries, between 6.3 and 4.72 Ma. It is clear that the younger series is dominated by the 100-kyr cycle while the 23-kyr cycle dominates the older one.

COMPARISON WITH THE STABLE ISOTOPIC RECORD

A detailed record of the late Miocene variations of the $\delta^{18}\text{O}$ and $\delta^{13}\text{C}$ in planktonic and benthic foraminifera from DSDP hole 552A has been established by Keigwin et al. [1986] and Keigwin [1987]. The $\delta^{18}\text{O}$ record reveals two significant enrichments in the $\delta^{18}\text{O}$ in both planktonic and benthic foraminifera at ~4.94 Ma and at ~5.22 Ma. These are interpreted as reflecting glacial

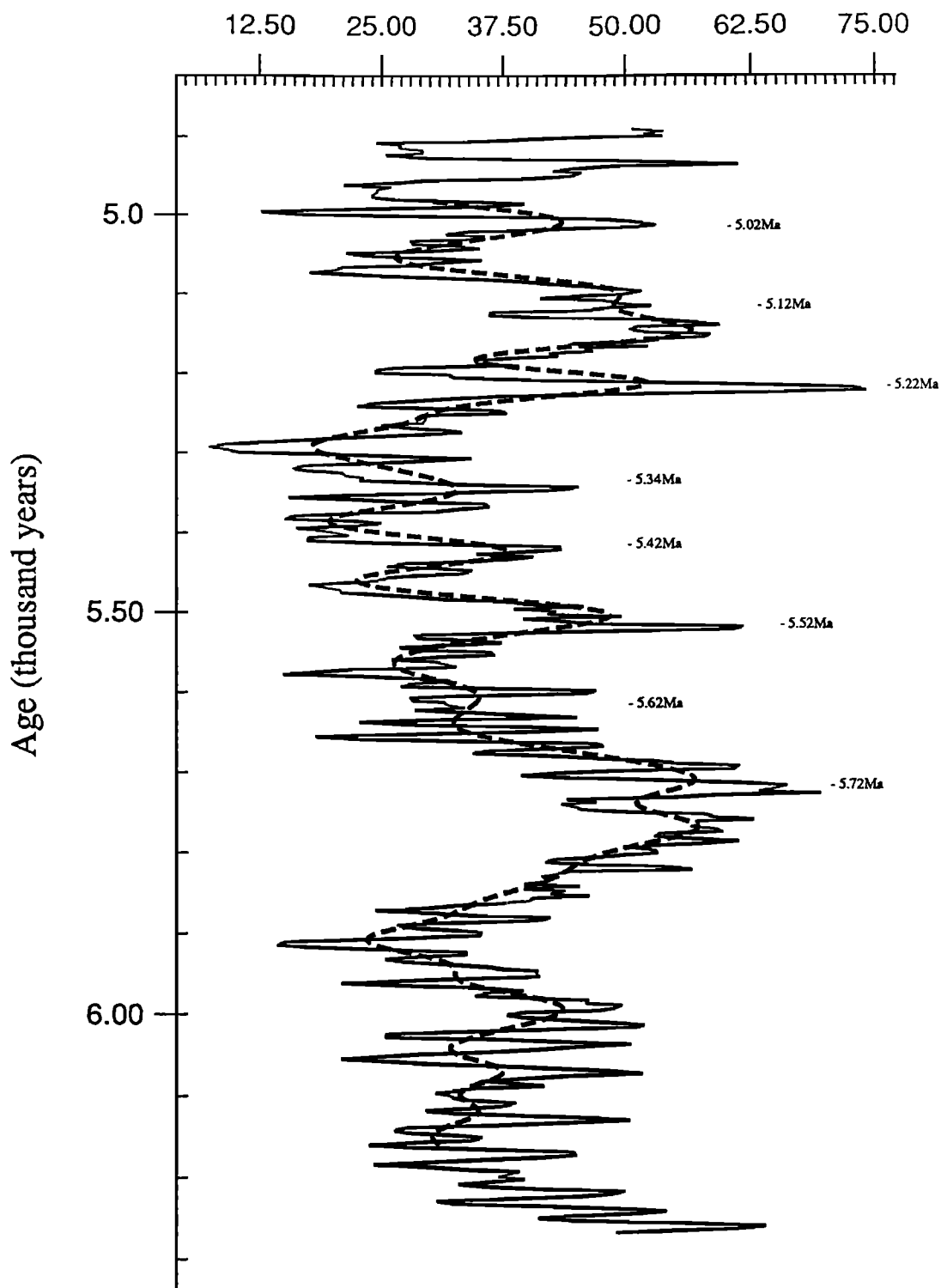


Fig. 4. Fluctuations in abundance of *Coccolithus pelagicus* versus *Reticulofenestra pseudoumbilica* during the late Miocene in the North Atlantic (DSDP hole 552A). Solid line: 3-point moving average. Dashed line, low-pass filtering cutting at 1/60; this line visualizes the strength and regularity of the frequency 1/100 in the upper part of the series.

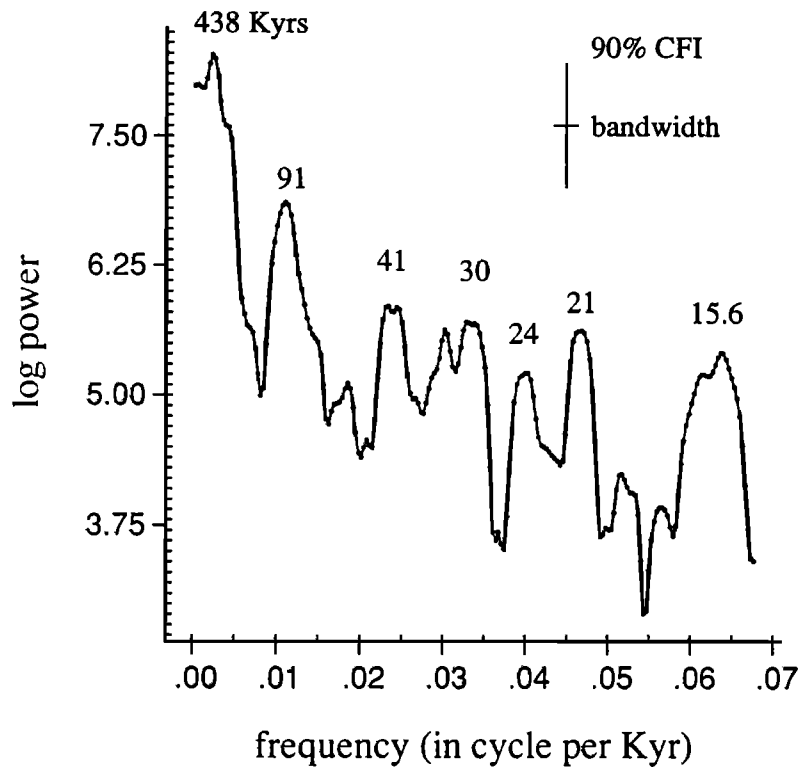


Fig. 5. Log of the power spectral density in the Cp/Rp series.

TABLE 4. Periods Revealed Through Spectral Analysis of the Cp/Rp

Observed, kyr	Interpretation	Band of Filtering	Percent of the Total Variance of Filtered Series
438	eccentricity?	>200	51
91	eccentricity	100	46
41	obliquity	40	14
30	non linearity		
24	precession	22	11
21	precession		
15.6	non linearity		

maxima which may have resulted in 60 m sea level lowerings [Keigwin et al., 1986]. The $\delta^{13}\text{C}$ record indicates that brief minima and a $\delta^{13}\text{C}$ shift occurred around 5.4 and 6 Ma, respectively.

The samples used to establish the Cp/Rp record are also those which served for establishing the isotopic record. Direct comparison between the two records is

therefore possible (Figures 8 and 9). The dramatic increases in abundance in *C. pelagicus* at 4.7 and 5.22 Ma (at 106 and 119 mbsf, respectively, in the hole, Figure 2) are exactly correlative with the late Miocene ice build up related $\delta^{18}\text{O}$ enrichments (Figure 8). Spectral analysis on the $\delta^{18}\text{O}$ series has been performed in order to verify whether orbital forcing drives $\delta^{18}\text{O}$ variations. The log of the

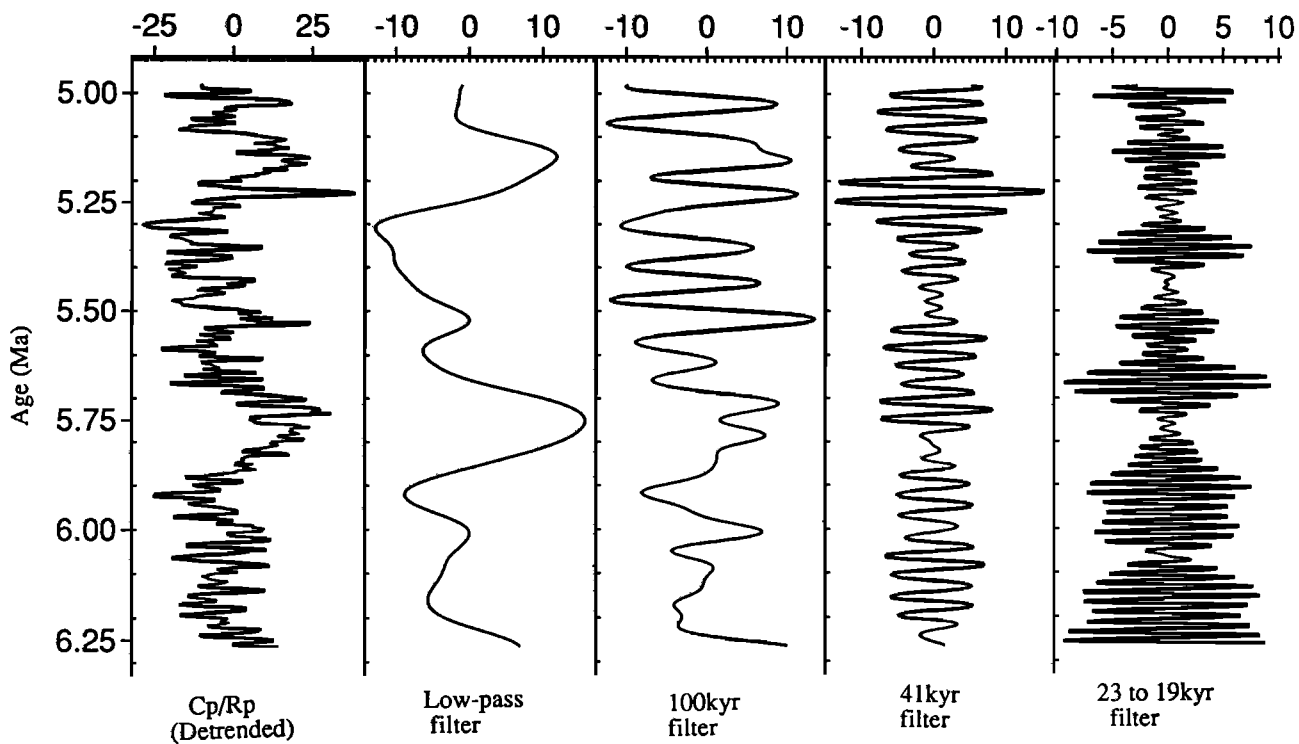


Fig. 6. Filtered Cp/Rp series. Shown from left to right are the detrended Cp/Rp series, low-pass filtered Cp/Rp signal, band-pass filtered Cp/Rp signal at 100, 41, and 19-23 kyr.

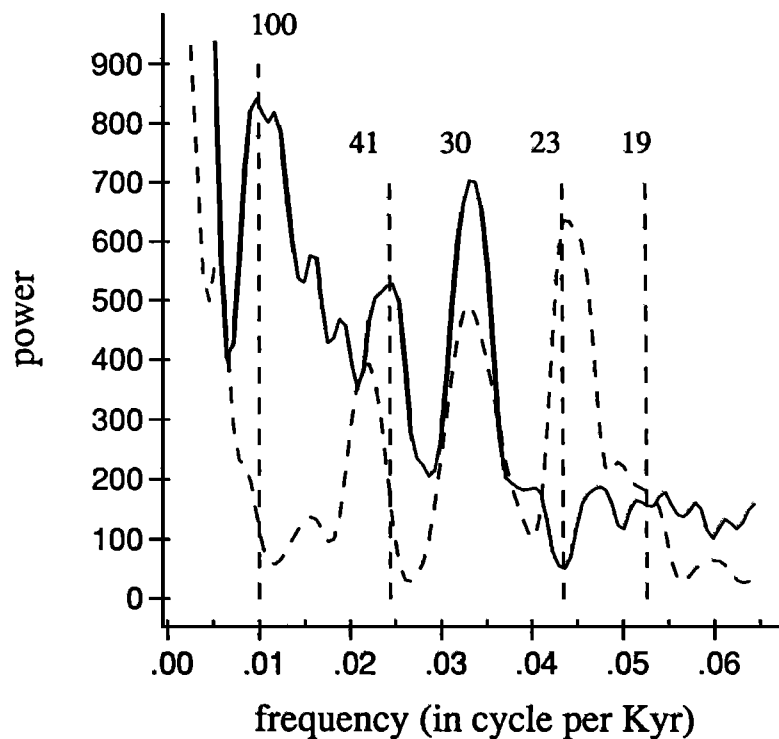


Fig. 7. Comparison of the spectral density power of the younger (5.72-4.89 Ma) and the older (6.3-4.72 Ma) parts of the series. Band-width is 0.005. Vertical dashed lines indicate the expected Milankovitch frequencies. See text for further explanation.

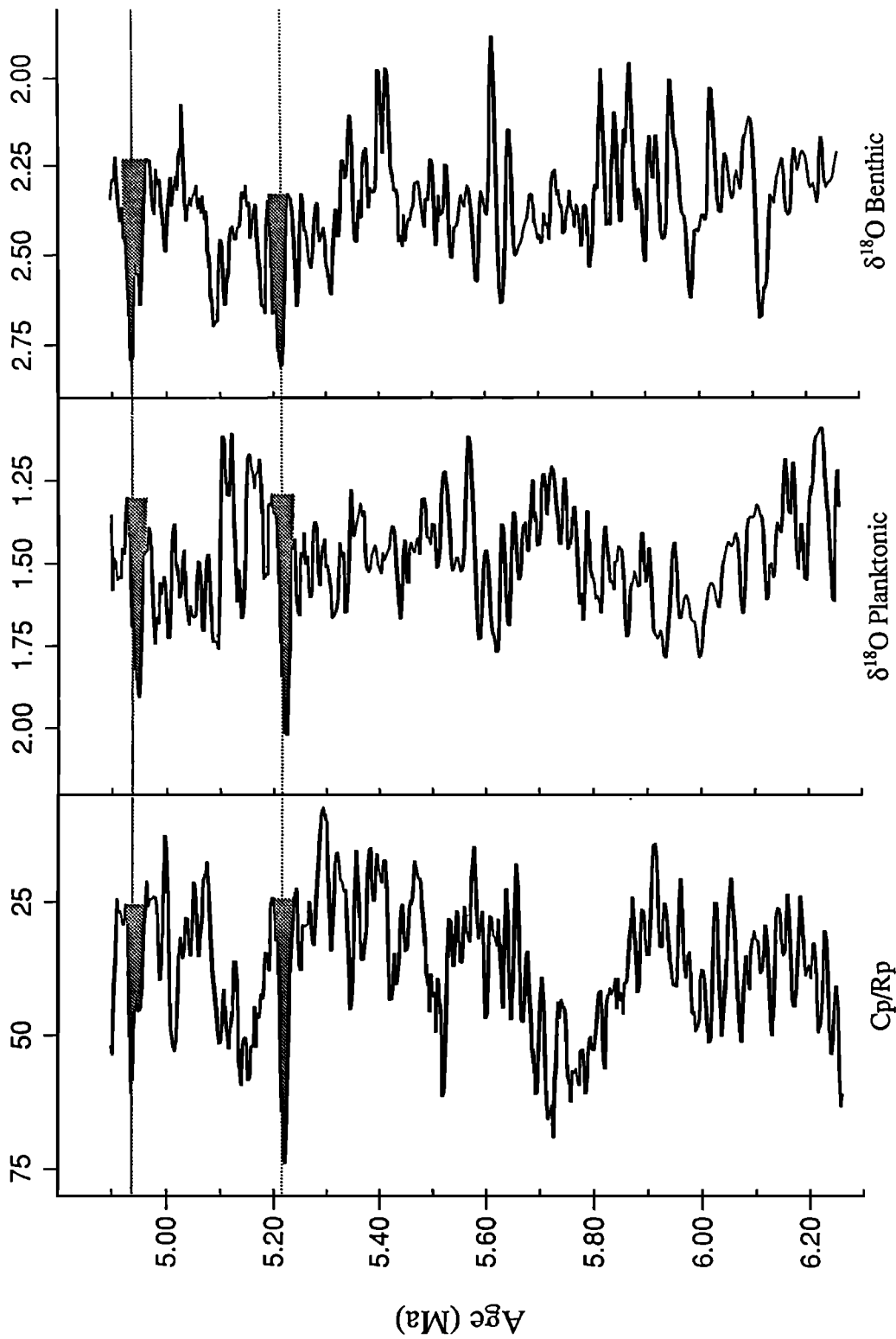


Fig. 8. Comparison of the Cp/Rp series with the $\delta^{18}\text{O}$ signals from planktonic and benthic foraminifera (isotopic data from Keigwin et al. [1986] and Keigwin [1987]). Shaded areas are major increases in $\delta^{18}\text{O}$ interpreted as reflecting glacial events [Keigwin et al., 1986; Keigwin, 1987]; these correlate precisely with sharp increases in abundance of *C. pelagicus*.

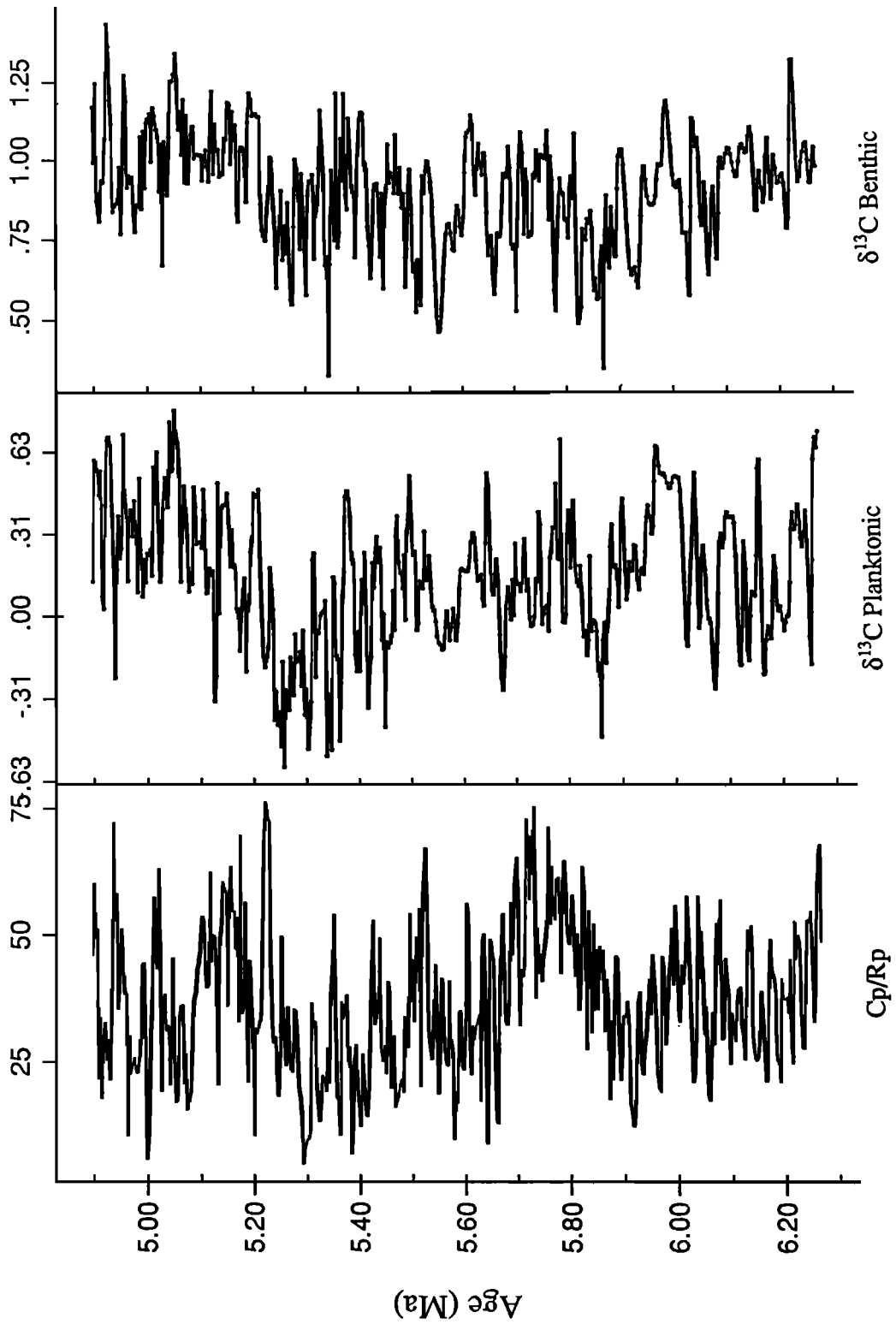


Fig. 9. Comparison of the Cp/Rp series with the $\delta^{13}\text{C}$ signals from planktonic and benthic foraminifera (isotopic data from Keigwin et al. [1986] and Keigwin [1987]).

power spectral density in the planktonic foraminifera $\delta^{18}\text{O}$ series (Figure 10) yields power at 236, 85, 39, 28, and 20 kyr with a large peak only for the latter. The 39-kyr period may represent the obliquity cycle, and the 20-kyr period may represent the precession cycle. It is difficult to identify the 85-kyr period as the eccentricity cycle. This latter cycle is not emphasized in the frequency domain, and in addition, the series does not show striking variations in the order of 100 kyr in the time domain. Below the Matuyama, this period is not present in Pliocene $\delta^{18}\text{O}$ records [Ruddiman et al., 1986].

No clear correlations can be established between the Cp/Rp variations and the $\delta^{13}\text{C}$ curve [Keigwin et al., 1986; Keigwin, 1987] except at two levels. The $\delta^{13}\text{C}$ minimum which occurs at ~155 mbsf (~6 Ma) and the brief minima which occur between 120 and 125 mbsf (~5.4 Ma) correlates with lower values of the Cp/Rp.

DISCUSSION

The fact that the Cp/Rp series yields the Milankovitch periods suggests that the variations in relative abundance between *Coccolithus pelagicus* and *Reticulofenestra pseudumbilica* during the late Miocene were strongly related to climatic variations. As for other members of the phytoplankton, the growth and the geographic and seasonal distribution of the coccolithophorids are primarily controlled by environmental factors, in particular, temperature and concentration in nutrients (see discussion by Raymont [1980]).

The present distribution of *Coccolithus pelagicus* is narrowly controlled by temperature. This extant species is restricted to high latitudes where it is known from the North Atlantic [McIntyre and Bé, 1967], the North Pacific [Geitzenauer et al., 1976] and the South Pacific [Nishida, 1979]. Okada and McIntyre [1979] established that its temperature range is 0-15°. The ecologic affinities of *C. pelagicus* may have changed through the Cenozoic, but Haq [1980, p. 422] indicated that the paleogeographic distribution of *C. pelagicus* through the Miocene "shows similarities to the modern biogeographic distribution of this taxon". The restriction of *C. pelagicus* to cold water masses has been well-illustrated by Bukry [1980], who showed that in the eastern Pacific Ocean, since the late Miocene, its abundance pattern does not follow a latitudinal gradient but is linked to the paths of cold water currents.

There seem to be no distinct ecologic preferences for the extinct species

Reticulofenestra pseudumbilica. Often regarded as cosmopolitan [e.g., Bukry, 1972, 1976], it has been suggested to have had tolerance for cold waters [Wise, 1976]. Haq [1980, Figure 7] shows, however, that in the North Atlantic, during the Neogene, *R. pseudumbilica* was most abundant at mid-latitudes.

Based on these data, it can be inferred that variations of the Cp/Rp at a given site reflect water masses movements. A high Cp/Rp (*C. pelagicus* abundant) indicates a cold water mass; a low Cp/Rp indicates a more temperate water mass. The validity of this inferred relationship is demonstrated by the high Cp/Rp values at 5.22 and 4.93 Ma, at times when peaks in $\delta^{18}\text{O}$ values correlate exactly with abundance peaks of *C. pelagicus*. The Cp/Rp is not linked exclusively with temperature, however, since there is no good correlation between the Cp/Rp and the $\delta^{18}\text{O}$ curve except at the levels cited above. Of the many ecologic parameters involved in regulating the growth of phytoplankton (see reviews by Raymont [1980] and Tappan [1980]), concentration in nutrients has a dominant effect [e.g., Rhee and Gotham, 1981]. Yet there is no clear correlation between the Cp/Rp and the $\delta^{13}\text{C}$ variations at DSDP site 552A, except at two levels. The correlation between $\delta^{13}\text{C}$ minima and low Cp/Rp ratio suggests that increase in abundance of *R. pseudumbilica* may reflect seawater chemical changes.

It is interesting to note that the Cp/Rp curve reflects the global late Miocene paleoclimatic and paleoceanographic changes as deciphered through isotopic studies. The $\delta^{18}\text{O}$ enrichments at DSDP site 552A represent increases in ice volume. The $\delta^{13}\text{C}$ minimum at ~155 mbsf at DSDP site 552A corresponds to the late Miocene $\delta^{13}\text{C}$ shift, and the brief minima between 120 and 125 mbsf correlate with minima at DSDP site 588 [Keigwin, 1987]. However, only at times of major global changes is there a good correlation between the Cp/Rp and the isotopic curves. This indicates that the Cp/Rp yields a complex paleoclimatic/paleoceanographic message. It will require similar detailed studies at different locations to understand it.

A change in regime occurs at 5.72 Ma (Figure 7) from a series dominated by a 20-kyr cycle to a series dominated by a 100-kyr cycle. This shift may result either from a change in the nature of the forcing agent itself or from a change in the nature of the response to this forcing agent. A similar shift in spectral power (from a 41-kyr dominated series to a 100-kyr dominated series) occurs in

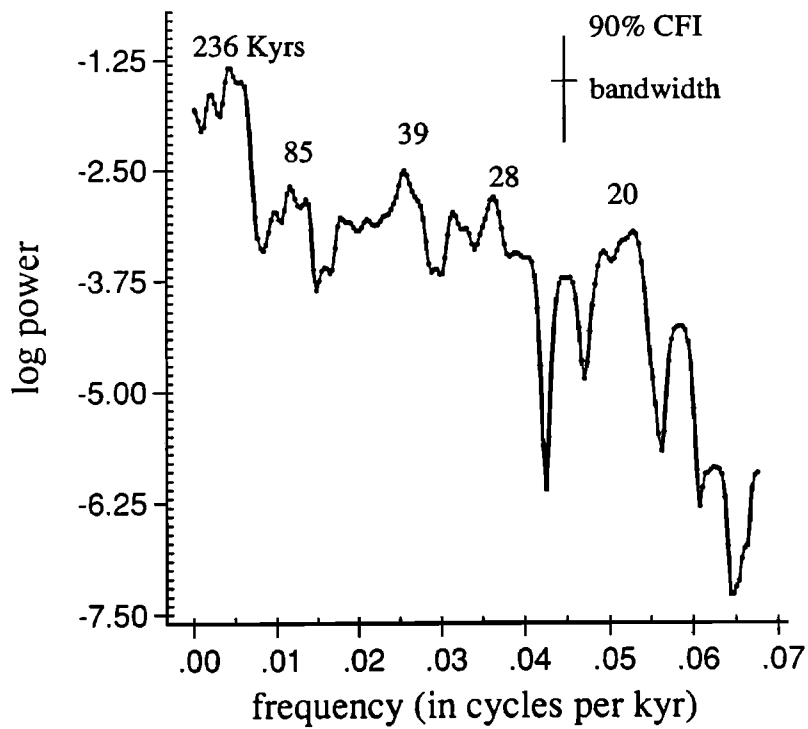


Fig. 10. Log of the power spectral density in the $\delta^{18}\text{O}$ record from planktonic foraminifera.

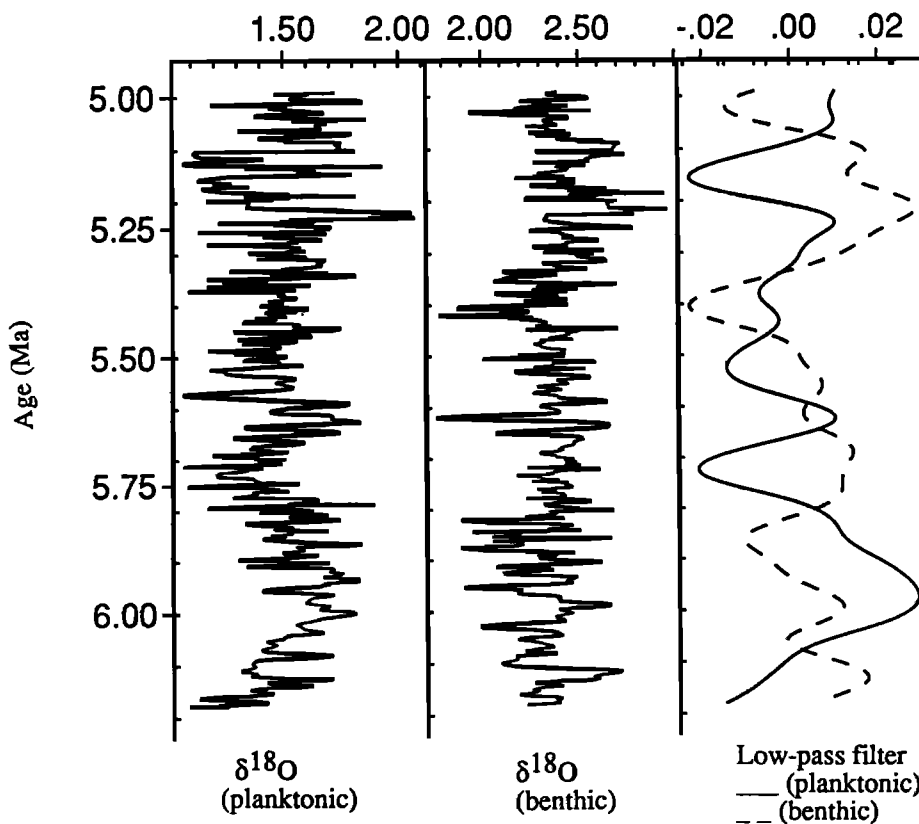


Fig. 11. Low-pass-filtered $\delta^{18}\text{O}$ signal from planktonic (solid line) and benthic (dashed line) foraminifera.

Pleistocene $\delta^{18}\text{O}$ series [e.g., Pisias and Moore, 1981; Ruddiman et al., 1989]. The dominance of the 100-kyr cycle in the late Pleistocene has been ascribed to nonlinear feedbacks resulting from different time constants of the decay and growth of ice sheets [Imbrie and Imbrie, 1980]. However, the reason for the spectral shift remains unclear, and it has been suggested that the shift was tectonically driven, the rising of mountains modifying atmospheric circulation so that greater cooling occurred over larger areas of Canada and North Europe [Ruddiman et al., 1989]. For these authors, the shift is neither orbital in origin nor resulting from ice sheets variations in the northern hemisphere.

The increase in the 100-kyr power and the concomitant decrease in the 20-kyr power at 5.72 Ma at DSDP site 552A is observed only in the Cp/Rp series. The $\delta^{18}\text{O}$ record, particularly that from the planktonic foraminifera, shows, instead, an increase in the amplitude of the 20-kyr cycle (Figures 11 and 12). The presence of a strong 30-kyr cycle in the Cp/Rp curve suggests a nonlinear response of the calcareous nannofossils (and of the water

mass movements) to climatic changes. Like the 30-kyr cycle, the 100-kyr cycle may result from this nonlinearity. The decrease of the 20-kyr cycle may be explained by the fact that the large amplitude of the 100-kyr signal hides signals of smaller amplitude at higher frequencies. The filtered Cp/Rp series (Figure 6) shows a general increase in amplitude through time. The same increase is seen in the filtered $\delta^{18}\text{O}$ series (Figure 12).

Hodell et al. [1989] observed that the $\delta^{18}\text{O}$ records from benthic foraminifera from Moroccan sections are characterized by a significant increase in amplitude in frequency of the signal during an interval which corresponds to the Messinian salinity crisis (between 5.5 and 4.8 Ma). According to Hodell et al. [1989, p. 478], this trend is a "ubiquitous feature of many deep sea carbonate records during the late Miocene". These increases are also correlative with the increase in amplitude of the 100-kyr cycle in the Cp/Rp series. The importance of climatic fluctuations during the late Miocene is emphasized by the occurrence of two major $\delta^{18}\text{O}$ events linked to glacial intensification.

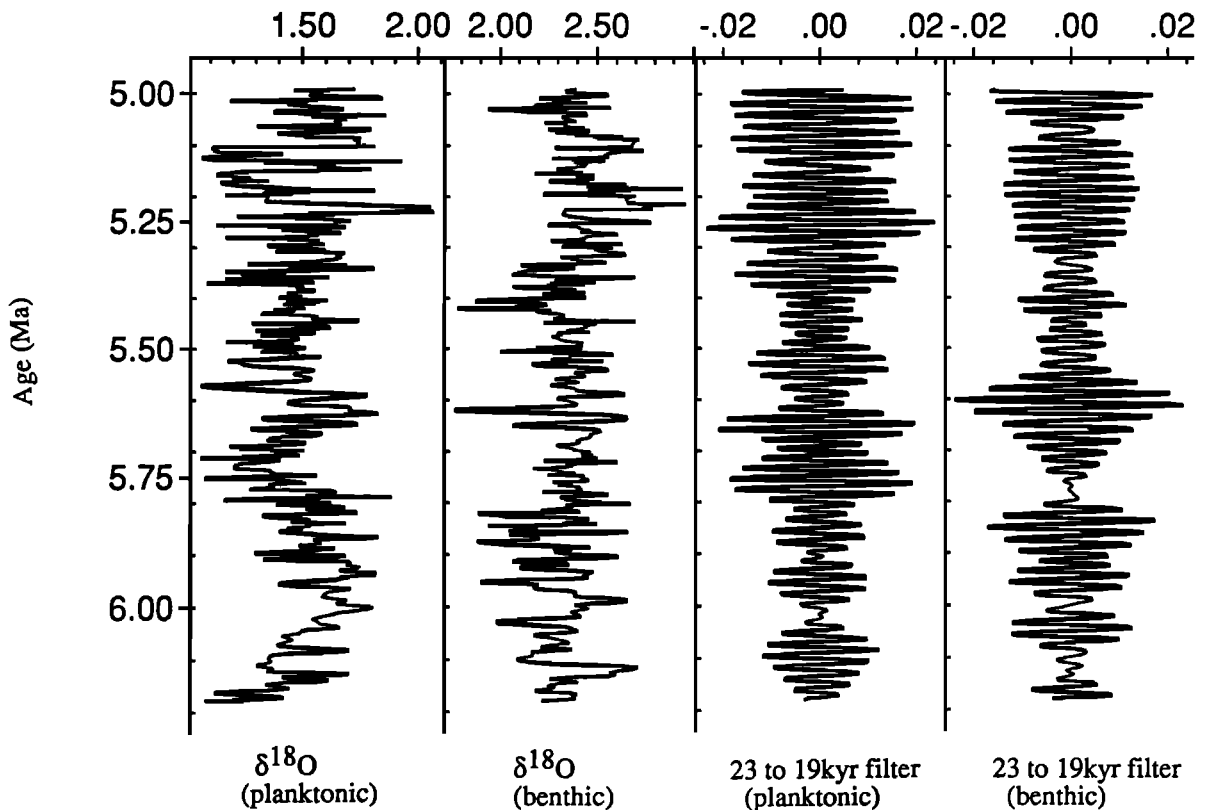


Fig. 12. Filtered $\delta^{18}\text{O}$ signal from planktonic and benthic foraminifera: (Left) $\delta^{18}\text{O}$ records; (Right) band-filtered $\delta^{18}\text{O}$ signals at 23-19 kyr.

Acknowledgments. We are thankful to L. D. Keigwin for providing samples from DSDP site 552A and for sharing the isotopic data from this site; to him and to P. Andreieff, W. A. Berggren, T. D. Herbert, and E. Vincent for helpful discussions and for reviewing early versions of this manuscript; and to two anonymous reviewers of the paper. We are particularly grateful to J. Imbrie for his kind guidance. Financial support from the Bureau de Recherches géologiques et minières is gratefully acknowledged. This is Woods Hole Oceanographic Institution contribution 7620.

REFERENCES

- Backman, J., Cenozoic calcareous nannofossil biostratigraphy from the northeastern Atlantic Ocean-Deep Sea Drilling Project, leg 81, *Init. Rep. Deep Sea Drill. Proj.*, 81, 403-428, 1984.
- Backman, J., and P. Pestiaux, Pliocene *Discoaster* abundance variations, Deep Sea Drilling Project site 606: Biochronology and paleoenvironmental implications, *Initial Rep. Deep sea Drill. proj.*, 94, (2), 903-910, 1987.
- Backman, J. and N. J. Shackleton, Quantitative biochronology of Pliocene and early Pleistocene calcareous nannofossils from the Atlantic, Indian and Pacific oceans, *Mar. Micropaleontol.*, 8, 141-170, 1983.
- Backman, J., P. Pestiaux, H. Zimmerman, and O. Hermelin, Palaeoclimatic and palaeoceanographic development in the Pliocene North Atlantic: *Discoaster* accumulation and coarse fraction data, North Atlantic Palaeoceanography, edited by Summerhayes, C. P. and N. J. Shackleton, *Geol. Soc. Spec. Publ. London*, 21, 231-242, 1986.
- Badlauf, J., Cenozoic calcareous nannofossil biostratigraphy from the Rockall Plateau region, North Atlantic, Deep Sea Drilling Project, leg 81, *Initial Rep. Deep Sea Drill. Proj.*, 81, 439-478, 1984.
- Beaufort, L., Concept of species in the genus *Reticulofenestra*, paper presented at INA Meeting, International Nannopaleontologists Association, Florence, 1989.
- Berggren, W. A., D. V. Kent, and J. A. Van Couvering, Neogene geochronology and chronostratigraphy, *Geochronology of the Geological Record*, edited by N.J. Snelling, *Geol. Soc. London Mem.* 10, 211-260, 1985.
- Broecker, W. S., Glacial to interglacial changes in the ocean chemistry, *Prog. Oceanogr.*, 11, 151-197, 1982.
- Bukry, D., Coccolith stratigraphy leg 6, Deep Sea Drilling Project, *Initial Rep. Deep Sea Drill. Proj.*, 6, 965-1004, 1971.
- Bukry, D., Further comments on coccolith stratigraphy, leg 12, Deep Sea Drilling Project, *Initial Rep. Deep Sea Drill. Proj.*, 12, 1071-1083, 1972.
- Bukry, D., Silicoflagellate and coccolith stratigraphy, Norwegian Greenland Sea, Deep Sea Drilling Project leg 38, *Initial Rep. Deep Sea Drill. Proj.*, 38, 843-855, 1976.
- Bukry, D., Coccolith stratigraphy, tropical eastern Pacific Ocean, Deep Sea Drilling Project leg 54, *Initial Rep. Deep Sea Drill. Proj.*, 54, 535-543, 1980.
- Channell, J. E. T., D. Rio, and R. C. Thunell, Miocene/Pliocene boundary magnetostratigraphy at Capo Spartivento, Calabria, Italy, *Geology*, 16, 1096-1099, 1988.
- Chepstow-Lusty, A., J. Backman, and N.J. Shackleton, Comparison of upper Pliocene *Discoaster* abundance variations from North Atlantic sites 552, 607, 658, 659, and 662: Further evidence for marine plankton responding to orbital forcing, *Proc. Oc. Drill. Program, Scientific results*, 108, 121-141, 1989.
- Driever, B., Calcareous nannofossil biostratigraphy and paleoenvironmental interpretation of the Mediterranean Pliocene, *Utrecht Micropaleont. Bull.*, 36, 1-245, 1988.
- Geitzenauer, K. R., M. B. Roche, and A. McIntyre, Modern Pacific coccolith assemblages: Derivation and application to late Pleistocene paleotemperature analysis, *Mem. Geol. Soc. Amer.* 145, 423-448, 1976.
- Haq, B. H., Biogeographic history of Miocene calcareous nannoplankton and paleoceanography of the Atlantic Ocean, *Micropaleontology*, 26 (4), 414-443, 1980.
- Haq, B. U., and W. A. Berggren, Late Neogene calcareous plankton biochronology of the Rio Grande Rise (South Atlantic Ocean), *J. Paleontol.*, 52, 1167-1194, 1978.
- Haq, B. U., and G. P. Lohmann, Early Cenozoic calcareous nannoplankton biogeography of the Atlantic Ocean, *Mar. Micropaleontol.*, 1, 119-194, 1976.
- Haq, B. H., I. Premoli-Silva, and G. P. Lohmann, Calcareous plankton paleobiogeographic evidence for major climatic fluctuations in the early

- Cenozoic ocean, *J. Geophys. Res.*, **82**, 27,3861-3876, 1977.
- Hodell, D. A., and J. P. Kennett, Late Miocene-early Pliocene stratigraphy and Paleoceneanography of the South Atlantic and southwest Pacific oceans: A synthesis, *Paleoceanography*, **1**, 285-311, 1986.
- Hodell, D. A., R. H. Benson, J. P. Kennett, and K. Rakic-El-Bied, Stable isotope stratigraphy of latest Miocene sequences in northwest Morocco: The Bou Regreg section, *Paleoceanography*, **4**, 407-482, 1989.
- Hsü, K. J., M. B. Cita, and W. B. F. Ryan, The origin of the Mediterranean evaporites, *Initial Rep. Deep Sea Drill. Proj.*, **13**, 623-636, 1973.
- Imbrie, J., and J. Z. Imbrie, Modeling the climate response to orbital variations, *Science*, **207**, 943-953, 1980.
- Keigwin, L. D., Toward a high-resolution chronology for latest Miocene paleoceanographic events, *Paleoceanography*, **2**, 639-660, 1987.
- Keigwin, L. D., M.-P. Aubry, and D. V. Kent, North Atlantic late Miocene stable-isotope stratigraphy, biostratigraphy, and magnetostratigraphy, *Initial Rep. Deep Sea Drill. Proj.*, **94**, 935-963, 1986.
- Kennett, J. P., Recognition and correlation of the Kapitean Stage (upper Miocene, New Zealand), *N. Z. J. Geol. Geophys.*, **10**, 1051-1063, 1967.
- Le Treux, H., J. Jouzel, and M. Ghil, Isotopic modeling of climatic oscillations: Implications for a comparative study of marine and ice core records, *J. Geophys. Res.*, **93**, 9365-9383, 1988.
- Lohmann, G. P., and J. J. Carlson, Oceanographic significance of Pacific late Miocene calcareous nannoplankton, *Mar. Micropaleontol.*, **6**, 553-579, 1981.
- McIntyre, A., and A. W. H. Bé, Modern Coccolithophoridae of the Atlantic Ocean, I, Placoliths and cyrtoliths, *Deep Sea Res.*, **14**, 561-597, 1967.
- Nesteroff, W. D., et al., Evolution de la sédimentation pendant le Néogène en Méditerranée d'après les forages JOIDES-DSDP, in *The Mediterranean Sea*, edited by D.J. Stanley, pp. 47-62, Dowden, Hutchinson and Ross, Stroudsburg, Pa., 1972.
- Nishida, S., Atlas of Pacific Nannoplankton, *News of Osaka Micropaleont.*, sp. paper **3**, 1-31, 1979.
- Okada, H., and A. McIntyre, Seasonal distribution of the modern coccolithophores in the Western North Atlantic Ocean, *Marine Biology*, **54**, 319-328, 1979.
- Perch-Nielsen, K., Cenozoic calcareous nannofossils, edited by H. M., Bolli, J. B. Saunders, and K. Perch-Nielsen, *Plankton Stratigraphy*, pp 427-559, Cambridge University Press, New York, 1985.
- Pisias, N. G., and T. C. Moore, Jr., The evolution of the Pleistocene climate: A time series approach, *Earth Planet Sci. Lett.*, **52**, 450-458, 1981.
- Pisias, N. G., and D. K. Rea, Late Pleistocene paleoclimatology of the central equatorial Pacific: Sea surface response to the southeast trade winds, *Paleoceanography*, **3**, 21-37, 1988.
- Pujos, A., Nannofossils from Quaternary deposits in the high productivity area of the central equatorial Pacific, Deep Sea Drilling Project Leg 85 *Init. Rept. Deep Sea Drill. Proj.*, **85**, 553-579, 1985.
- Pujos, A., Late Eocene to Pleistocene medium-sized and small-sized reticulofenestrids, *Abh. Geol. Bundesanst. Austria*, **39**, 239-277, 1987.
- Raymont, J. E. G., *Plankton and Productivity in the Oceans*, Pergamon, New York, 1980.
- Rhee, G.-Y., and I.J. Gotham, The effect of environmental factors on phytoplankton growth: Temperature and the interactions of temperature with nutrient limitation, *Limnol. Oceanogr.*, **26**, 635-648, 1981.
- Roberts, D. C., et al., Sites 552-553, *Initial Rep. Deep Sea Drill. Proj.*, **81**, 31-233, 1984.
- Ruddiman, W.F., M. Raymo, and A. McIntyre, Matuyama 41,000-year cycles: North Atlantic Ocean and northern hemisphere ice sheets, *Earth Planet. Sci. Lett.*, **80**, 117-129, 1986.
- Ruddiman, W.F., M. Raymo, D. G. Martinson, B. M. Clement and J., Backman, Pleistocene evolution: Northern hemisphere ice sheets and North Atlantic Ocean, *Paleoceanography*, **4**, 353-412, 1989.
- Ryan, W. B. F., M. B. Cita, M. D. Rawson, L. H. Burckle, and T. Saito, A paleomagnetic assignment of Neogene stage boundaries and the development of isochronous datum planes between the Mediterranean, the Pacific and Indian oceans in order to investigate the response of the world ocean to the Mediterranean salinity crisis, *Riv., Ital. Paleontol.*, **80**, 631-687, 1974.
- Schmidt, R. R., The calcareous nannofossils in the Potamidha section, *Utrecht Micropaleontol. Bull.*, **21**, 167-191, 1979.

- Shackleton, N. J., and J. P. Kennett, Late Cenozoic oxygen and carbon isotopic changes at DSDP Site 284: Implications for glacial history of the Northern Hemisphere and Antarctica, *Initial Rep. Deep Sea Drill. Proj.*, 29, 801-807, 1975.
- Shackleton, N.J., et al., Oxygen isotope calibration of the onset of ice rafting and history of glaciation in the North Atlantic region, *Nature*, 307, 620-623, 1984.
- Shumway, R.H., (Ed.), *Applied Statistical Time Series Analysis*, 379 pp., Prentice-Hall, Englewood Cliffs, N.J., 1988.
- Tappan, H., *The Paleobiology of the Plant Protists*, 1028 pp., W.H., Freeman, New-York, 1980.
- Thunell, R. C., Late Miocene-early Pliocene planktonic foraminiferal biostratigraphy and paleoceanography of low latitude marine sequences, *Mar. Micropaleontol.*, 6, 71-92, 1981.
- Wise, S. W., Calcareous nannofossils from cores recovered during leg 18, Deep Sea Drilling Project: Biostratigraphy and observations of diagenesis, *Initial Rep Deep Sea Drill. Proj.*, 18, 569-615, 1976.
- Zijderveld, J. D. A., J. W. Zachariasse, P. J. J. M. Verhallen, and F. J. Hilgen, The age of the Miocene-Pliocene boundary, *Newsl. Stratigr.*, 16, 169-181, 1986.
-
- M.-P. Aubry and L. Beaufort, Centre de Paléontologie Stratigraphique et Paléocécologie (URA 11), Université Claude Bernard (Lyon I), 27-43 Bd. du 11 Novembre, 69622 Villeurbanne Cedex, France.

(Received December 1, 1989;
revised August 14, 1990;
accepted August 15, 1990.)